photonics

MDPI

Communication

High–Power 792 nm Fiber–Coupled Semiconductor Laser

Peng Liu [1], Wanggen Sun [2], Xiao Sun [1], Zhen Zhu [2], Huabing Qin [2], Jian Su [2], Chengcheng Liu [2], Wenjing Tang [1], Kai Jiang [1,*], Wei Xia [1,2,*] and Xiangang Xu [2,3]

[1] School of Physics and Technology, University of Jinan, Jinan 250022, China; 202021100182@stu.ujn.edu.cn (P.L.); sps_tangwj@ujn.edu.cn (W.T.)
[2] Shandong Huaguang Optoelectronics Co., Ltd., Jinan 250101, China; sunwanggen@inspur.com (W.S.); zhuzhen@inspur.com (Z.Z.); qinhb1@inspur.com (H.Q.); sujian@inspur.com (J.S.); liuchch@inspur.com (C.L.); xxuu@sdu.edu.cn (X.X.)
[3] Institute of Novel Semiconductors, Shandong University, Jinan 250100, China
* Correspondence: sps_jiangk@ujn.edu.cn (K.J.); sps_xiaw@ujn.edu.cn (W.X.)

Abstract: The pumping of Tm-doped crystal or fiber by a 792 nm semiconductor laser is an important way to generate a mid-infrared laser, which is widely used in various fields. In this paper, a high–power 792 nm fiber–coupled semiconductor laser module was successfully fabricated with the output power of 232 W at a 10 A continuous current and the electro-optic conversion efficiency of 48.6%. The laser module is coupled with 24 chips into a fiber by spatial multiplexing and polarization combination technology. For a single emitting laser chip, the continuous wave (CW) output power and threshold current are 10.45 W at 10 A and 1.55 A, respectively. A polarization as high as 94% can also be realized, which is more suitable for laser spatial beam combining. The laser module was aged for more than 4000 h at 12 A and 25 °C without obvious power degradation.

Keywords: 792 nm semiconductor laser; fiber–coupled; spatial multiplexing; polarization combination

check for updates

Citation: Liu, P.; Sun, W.; Sun, X.; Zhu, Z.; Qin, H.; Su, J.; Liu, C.; Tang, W.; Jiang, K.; Xia, W.; et al. High–Power 792 nm Fiber–Coupled Semiconductor Laser. *Photonics* **2023**, *10*, 619. https://doi.org/10.3390/photonics10060619

Received: 18 March 2023
Revised: 22 May 2023
Accepted: 24 May 2023
Published: 26 May 2023

1. Introduction

Semiconductor lasers have been widely regarded as a research hotspot due to their high efficiency, small size, light weight, long lifetime and easy integration. In recent years, high-quality semiconductor lasers with high power have been widely needed in industrial processing, intelligent sensing, medical health, a solid or fiber laser pumping source, etc. [1,2]. However, compared with gas lasers, solid-state lasers and fiber lasers, traditional semiconductor lasers have some disadvantages, such as poor spectral characteristics, poor beam quality, low output power and low brightness. At present, the research focus of high–power semiconductor lasers is how to improve the beam quality [3,4] while obtaining high–power and high-efficiency output. Coupling the laser beam into an optical fiber is a good solution; it can improve the output power while preserving the quality of the beam, as well as realize the flexible transmission of the laser. Thus, the semiconductor lasers using multi-chip coupling technology can better meet the application requirements.

The 3~5 μm mid-infrared laser is the most ideal atmospheric transmission window, which is widely used in the fields of air pollution monitoring, infrared imaging, sensing technology, surgery, free space communication, photoelectric countermeasures and other fields [5]. As the pump source of an optical parametric oscillator, the 792 nm fiber–coupled semiconductor laser module first pumps the thulium-doped fiber laser and then pumps the holmium-doped solid-state laser, which is the main method to produce a mid-infrared laser in 3~5 μm. The maximum intensity of thulium's absorption peak is near 792 nm and its line width is 20 nm, and using a 792 nm semiconductor laser to pump a thulium–doped fiber laser has the highest pumping efficiency. The 792 nm semiconductor laser chips and fiber−coupled semiconductor laser modules with high power, high efficiency and high reliability are the core components of many mid-infrared devices such as a mid–infrared

laser electro-optical countermeasure system, which has received extensive attention in the world [6,7].

In 2020, nLIGHT reported a 793 nm fiber–coupled semiconductor laser module, which coupled 24 × 793 nm chips into a 200 μm fiber. The output power and electro–optical conversion efficiency were 190 W and 45%, respectively [8]. Also in 2020, Coherent released a 790 nm laser chip with a 100 μm width and 3 mm cavity length; the output power was 5.6 W at a 5 A current. By coupling three 790 nm chips into a 100 μm fiber, they also realized the preparation of a 793 nm fiber–coupled semiconductor laser module, whose output power was 13.5 W at a 5 A working current, and the electro–optical conversion efficiency was 48% [9].

In this work, we first developed and grew the 792 nm laser epitaxial wafer based on InGaAsP/GaInP material through the MOCVD equipment; then, we fabricated the laser chip by photolithography, etching, PECVD, metal evaporation, alloying and dissociation processes. Finally, an optical system was designed to collimate the fast axis and slow axis of laser chips to realize the fiber coupling of 24 chips. The output power of the laser module is 232 W at a 10 A continuous current, corresponding to an electro–optic conversion efficiency of 48.6%.

2. Laser Module Design Simulation and Preparation

2.1. 792 nm Semiconductor Laser Structure Design

The structure of the 792 nm semiconductor laser is shown in Table 1. We designed the asymmetric structure of cladding layer composition (n-$Al_{0.1}Ga_{0.4}In_{0.5}P$/p-$Al_{0.2}Ga_{0.3}In_{0.5}P$), cladding layer thickness (n-1.5 μm/p-1 μm) and waveguide layer thickness (n-0.9 μm/p-0.45 μm). The middle layer is a compressively strained $In_{0.6}Ga_{0.4}As_{0.3}P$ quantum well with a strain value of 0.5%.

Table 1. Structure of 792 nm semiconductor laser.

Layer	Material	Thickness (nm)	Doping (cm^{-3})
Contact	GaAs	200	$>1 \times 10^{19}$
P-cladding	$Al_{0.2}Ga_{0.3}In_{0.5}P$	1000	1×10^{18}
P-waveguide	$Ga_{0.5}In_{0.5}P$	450	–
Quantum well	$In_{0.6}Ga_{0.4}As_{0.3}P$	9	–
N-waveguide	$Ga_{0.5}In_{0.5}P$	900	–
N-cladding	$Al_{0.1}Ga_{0.4}In_{0.5}P$	1500	1×10^{18}
Buffer	GaAs	200	2×10^{18}

Optical field distribution of the symmetric structure and asymmetric structure is shown in Figure 1. The pink line is the quantum well position, the black line is the symmetric waveguide boundary and the red line is the asymmetric waveguide boundary.

Compared with the traditional asymmetric structure laser [10], we not only realized the asymmetry between the composition and thickness of the cladding layer, but also reduced the thickness of the P-waveguide layer. By adopting the asymmetric wide waveguide structure, the light field distribution of the laser is changed from the symmetric distribution centered on the quantum well to the asymmetric distribution biased towards the N-type area, so as to reduce the overlapping ratio of the light field and the highly doped P-confinement layer. As a result, the internal loss and waste heat of the laser are reduced; meanwhile, the differential quantum efficiency and the reliability are improved [11].

The main factors that limit the output power of 792 nm semiconductor lasers are internal quantum efficiency and optical absorption, and the catastrophic optical damage of the cavity surface also has an important influence on the power and reliability of the laser [12]. The aluminum-containing active region of the traditional AlGaAs laser is prone to oxidation and dark-line defects, and the non-radiative recombination of carriers makes the cavity surface produce catastrophic optical damage, which limits the power and reliability

of the laser. Therefore, we designed the aluminum-free InGaAsP/GaInP active layer to make the laser have a high optical catastrophic power density on the cavity surface.

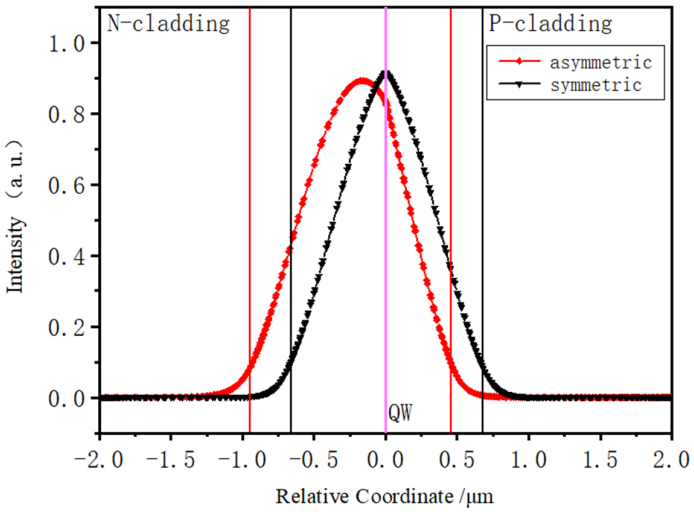

Figure 1. Optical field distribution of symmetric structure and asymmetric structure.

2.2. ZEMAX Simulation and Analysis

The ZEMAX software was used to simulate the spatial beam combining structure. Figure 2 gives the optical path of the fiber coupling module.

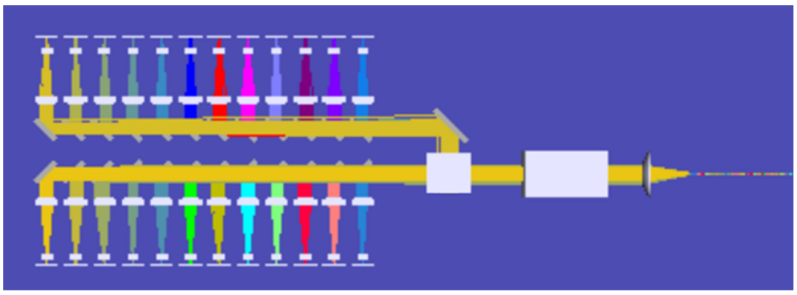

Figure 2. The optical path diagram of fiber coupling.

After polarization and beam combination, the beam becomes a rectangular parallel beam, as shown in Figure 3a, with a length of 5.04 mm and a width of 2.6 mm. Without changing the beam quality, the output power is doubled. A transform lens with the compression ratio of 0.4 and a focusing lens with focal lengths of 9 mm are used to converge the light spots, and for coupling into a 200 μm fiber. The transform lens is a combination of a convex lens and a concave lens. As shown in Figure 3b, the beam size of the fiber end face and the numerical aperture are 182 μm and 0.18, respectively.

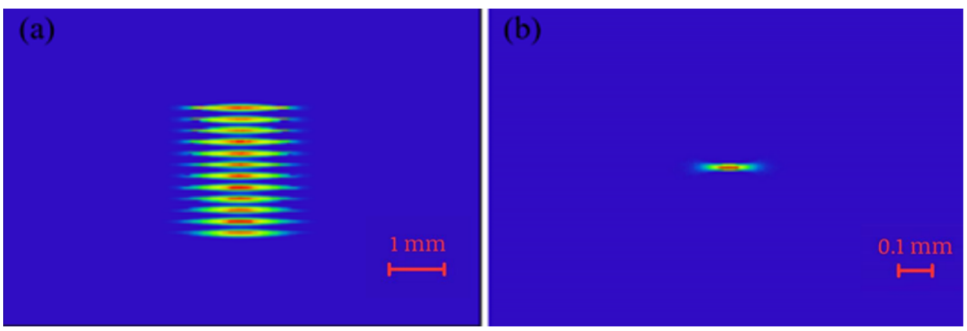

Figure 3. (**a**) Output profile after polarization combination; (**b**) focus laser beam.

2.3. Fiber−Coupled Laser Module Design and Preparation

The beam quality of the laser is calculated by the beam parameter product (*BPP*) [13], which can be expressed by the following formula:

$$BPP = \omega_0 \cdot \theta/2$$

where ω_0 is the waist radius of the laser spot, and θ is the far-field divergence angle. The *BPP* value is used to measure the quality of the semiconductor laser beam. The smaller the *BPP* value, the better the laser beam quality [14].

In this letter, a 200 μm fiber with a beam numerical aperture of 0.22 is selected. The divergence angle corresponding to the numerical aperture is 12.7°, and the radian value is 221 mrad, that is, ω_f = 100 μm and $\theta_f/2$ = 221 *mrad*. The BPP_F value of the optical fiber is

$$BPP_F = \omega_f \cdot \frac{\theta_f}{2} = 22.1\ mm \cdot mrad$$

Two conditions must be met when a light beam is coupled into a fiber—one is that the incident light spot size is less than the core diameter of the fiber, and the other is that the incident angle is less than the maximum incident light-receiving angle of the fiber.

The laser chip is bonded p-side down on the submount (AlN ceramic) by a die bonder system, and after the wire bonding process, the chip on the submount (COS) single emitter laser is completely fabricated. After a professional equipment test, the fast−axis divergence angle of the COS single-chip laser was 305 *mrad* (half angle), and the slow−axis divergence angle was 78.5 *mrad* (half angle). The area of the active area is 1 μm in the fast axis and 190 μm in the slow axis. The beam quality of the fast axis and slow axis is calculated as follows:

$$BPP_f = 1 \cdot \frac{10^{-3}}{2} \cdot 305 = 0.22\ mm \cdot mrad$$

$$BPP_s = \frac{0.19}{2} \cdot 78.5 = 7.46\ mm \cdot mrad$$

It can be seen that although the fast-axis divergence angle of the laser directly emitted by the semiconductor laser is very large, its *BPP* value is much smaller than that of the slow axis because of the small size of the active area. In order to obtain a high output power fiber-coupled module, the beams emitted by multiple semiconductor laser chips can be superimposed in the fast-axis direction and then coupled into the fiber.

The specific method is that we first horizontally solder 12 chips on the substrate according to the arithmetic progression, then collimate the fast axis and slow axis of the light beam with the collimating lens, compress the divergence angle, and achieve a nearly parallel light output. The fast-axis collimating lens is the FAC-300 lens of FISBA Company, with a focal length of 0.3 mm, numerical aperture of 0.7 and aspheric coefficient of −0.53. The divergence angle of the collimated beam in the fast-axis direction is 2.5 *mrad* (half angle), the reflector is 15 mm away from the laser cavity surface and the fast-axis spot size on the reflector is 333 μm. Considering the installation error, the step-height difference is set to 420 μm to avoid blocking the laser beam. After the laser beam is reflected by a 45° mirror, the height of the fast-axis beam is 4.95 mm. Then, the height of the beam is compressed into 1.98 mm by the transform lens with a compression ratio of 0.4. In the slow-axis direction, a cylindrical lens with a focal length of 12 mm is selected to collimate the laser beam, and after collimation, the remaining divergence angle of the slow axis is about 0.1°, and the spot width on the focusing mirror is 2.3 mm. The spot is coupled into a fiber using a focusing lens with a focal length of 9 mm and a numerical aperture of 0.3; the whole size of the end face spot of the fiber is 182 μm (full width), the incident angle is 20.6° (full angle) and the *BPP* value is 16.35 mm·mrad, which meets the coupling conditions of the fiber. The fiber coupling module structure is shown in Figure 4.

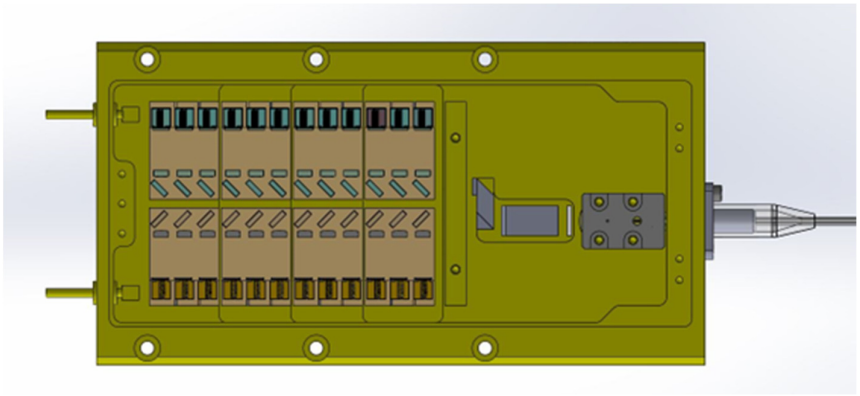

Figure 4. Fiber coupling laser module structure.

In order to further improve the output power of the coupled laser without affecting the beam quality, we divided 24 laser chips into two symmetrical groups, and combined the beams by polarization. The polarization beam combiner has the characteristics of transmitting P-polarized light and reflecting S-polarized light. As the outgoing lights of two groups of lasers are all P-polarized light, with the polarization beam combiner, one laser beam group is incident on the polarization beam combiner, and the other first passes through the 1/2 wave plate so that the polarization direction is rotated by 90° and P-polarized light becomes S-polarized light, which then enters the other side of the polarization beam combiner at 90° with the first group of lasers; it is thus reflected by the polarized beam combiner. This makes the two groups of laser beams superimposed together to improve the output power.

3. Experimental Results and Discussion

3.1. Single Emitter Semiconductor Laser Test Results

The curve of power and voltage versus current is shown in Figure 5. At a room temperature of 25 °C, the threshold current of single emitter COS (chip on the submount) is 1.55 A, and the threshold current density is 190 A/cm^{-2}. Under a 10 A current, the output power of the laser reaches 10.45 W, the voltage is 1.88 V, the electro−optical conversion efficiency is 55% and the polarization degree of the device is 94%. Compared with recent reports in the same spectral range [15], we not only achieved high power and high conversion efficiency, but also with increasing the working current, the laser still has no catastrophic optical damage at 20 A, which allows the laser to work at a higher current and higher power.

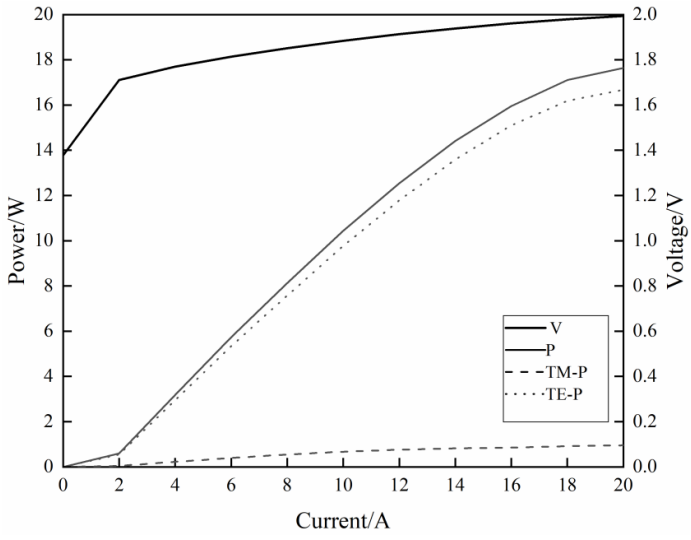

Figure 5. P-I-V curve of single emitter COS.

Figure 6a is the spectrum of the laser at 25 °C and a 10 A current. In the packaging process, with the increase of the number of single emitter lasers, the heat also increases, resulting in a red shift in wavelength. In order to meet the requirement of a 792 nm working wavelength of the packaged fiber coupling laser, a single emitter laser with a center wavelength of 789 nm and a full width half maximum (FWHM) of 2.3 nm is generally selected. The far-field characteristics of the laser are given in Figure 6b. The horizontal divergence angle is 9° and the vertical divergence angle is 35° at a 10 A working current.

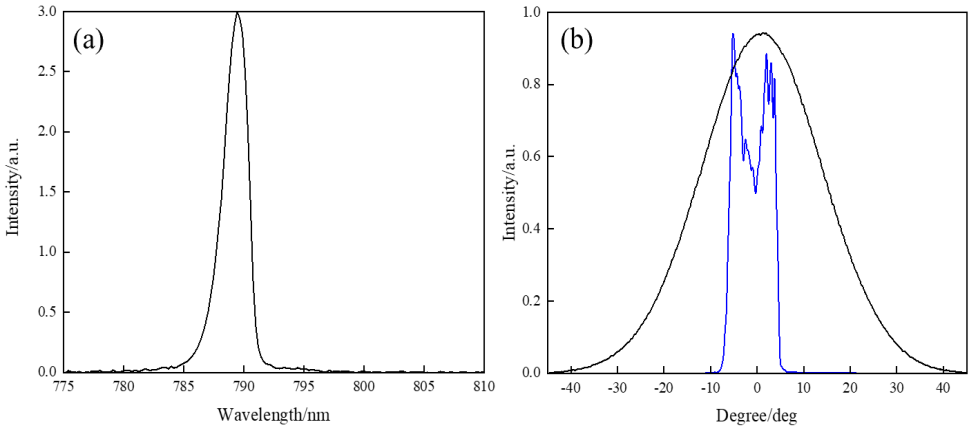

Figure 6. (**a**) Spectrum of single emitter COS; (**b**) Far-field profiles of single emitter COS.

All the diode laser devices discussed in this paper were fabricated in the same manner. We selected the COS single emitter laser with high consistency in the wavelength and power to make the fiber coupling module. As shown in Table 2, we selected the chips with an appropriate power and wavelength to make the fiber coupling module.

Table 2. Power and wavelength of 24 chips.

Number	Power (W)	Wavelength (nm)	Number	Power (W)	Wavelength (nm)
1	10.40	789.1	13	10.43	789.3
2	10.44	789.4	14	10.45	789.4
3	10.45	789.3	15	10.41	789.1
4	10.38	789.3	16	10.43	789.3
5	10.42	789.1	17	10.44	789.2
6	10.44	789.5	18	10.42	789.1
7	10.42	789.3	19	10.40	789.3
8	10.43	789.2	20	10.44	789.2
9	10.42	789.1	21	10.45	789.4
10	10.40	789.4	22	10.41	789.1
11	10.39	789.2	23	10.43	789.2
12	10.41	789.1	24	10.39	789.3

3.2. Test Results of Fiber Coupling Module

In the experiment, two cylindrical mirrors were used to compress the fast axis and slow axis of the laser module, and the output power was increased by polarization combining without reducing the beam quality. Finally, 24 single emitter semiconductor lasers were combined and coupled into a 200 μm fiber with a beam NA of 0.22. Figure 7 is the LIV curve of the fiber coupling semiconductor laser module. Under the condition of a 25 °C and 10 A continuous current test, the laser power reached 232 W, the slope efficiency was 27.44 W/A and the electro−optical conversion efficiency was 48.6%. As shown in Figure 8, the high power and high efficiency fiber coupling semiconductor laser module was prepared.

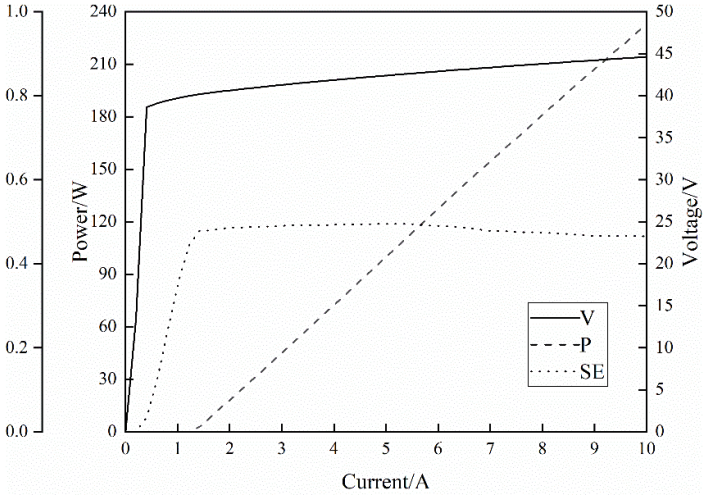

Figure 7. P-I-V curve of fiber coupling laser module.

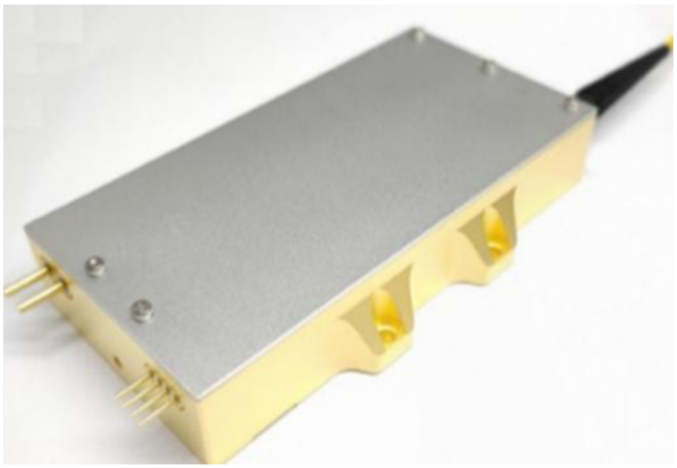

Figure 8. Fiber coupling laser module.

The spectrum of the fiber coupling laser module is shown in Figure 9. Using air cooling equipment, the peak wavelength is effectively controlled at 792 nm and the full width half maximum of the module is 3.86 nm under the working current of 10 A, which accords with the maximum absorption spectrum range of the Tm-doped fiber and can achieve the maximum pumping efficiency. Figure 10 shows the test curve of the divergence angle of the output beam from the fiber. The full divergence of 95% power is about 19.6°; the corresponding numerical aperture is 0.17. The beams of 24 single emitter lasers can be efficiently coupled into the 200 μm fiber through beam combining.

The 792 nm fiber coupling semiconductor laser is used as a pump source in mid-infrared laser applications, which requires high reliability. We integrated packaging of chips and mechanical structures, reduced the soldering hole and improved heat dissipation capacity, so as to obtain a high-reliability laser module [16]. In the experiment, we verified the reliable performance of the 792 nm laser module by increasing current (power) aging. The normal working current of the laser is 10 A. In view of the advantages of the Al-free structure laser designed by us in resisting the optical damage of the cavity surface, a current of 12 A is adopted for aging. Figure 11 shows the online monitoring aging curves of three groups of fiber coupling lasers with a water-cooling temperature of 25 °C. After aging for more than 4000 h, there is no obvious power degradation. The maximum power decrease is 1.62%, which meets the high-reliability requirements of the lasers.

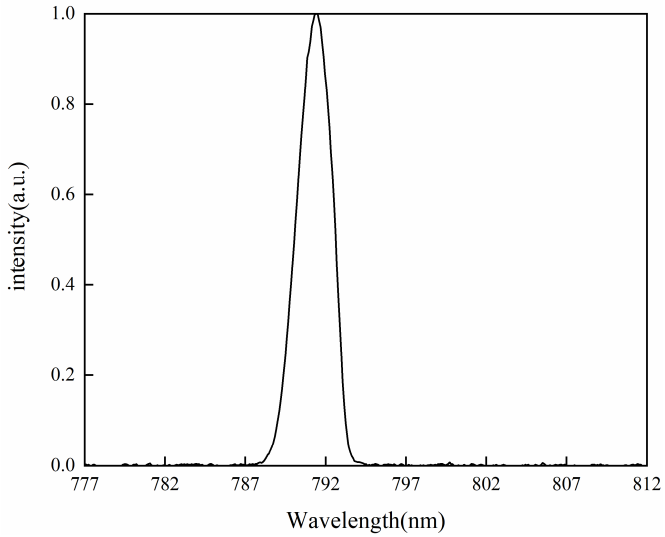

Figure 9. Spectrum of fiber coupling laser module.

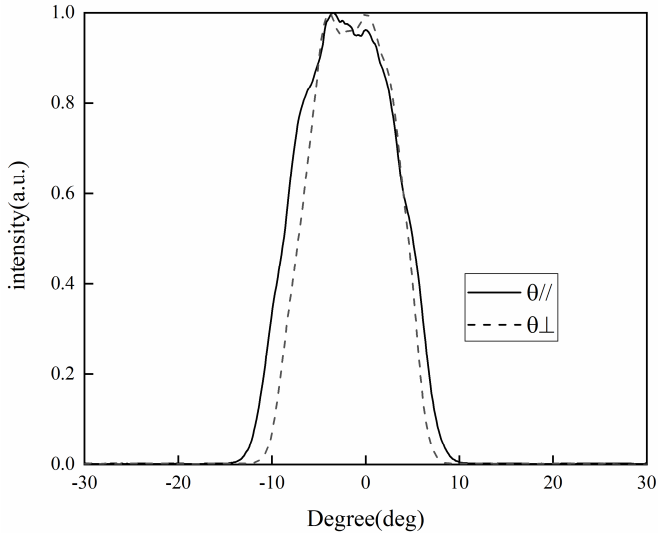

Figure 10. Divergence after beam combination.

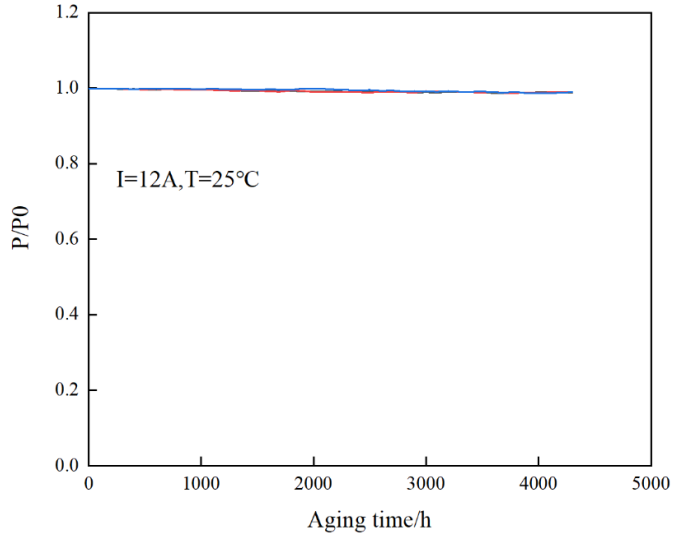

Figure 11. Life test of fiber coupling laser module at CW 25 °C 12 A.

4. Conclusions

We have developed a high-power 792 nm semiconductor laser module based on InGaAsP/GaInP material epitaxial growth, chip and packaging technology. The single emitter laser devices were tested at a 25 °C temperature, the output power reached 10.45 W at 10 A, the slope efficiency attained 1.3 W/A and the degree of polarization was 94%. Finally, the beams of 24 single emitter semiconductor lasers were coupled into a 200 μm fiber with the beam NA of 0.22. The coupling laser module output power reached 232 W and the electro−optical conversion efficiency was 48.6%; it also showed good reliability during the aging test. The developed 792 nm semiconductor laser modules have realized mass production and achieved good economic benefits.

Author Contributions: P.L. designed and performed the experiments, analyzed the data and drafted the manuscript; W.T. and X.S. helped with English writing; W.S. and K.J. fabricated and characterized the semiconductor laser; Z.Z. and C.L. performed the theoretical analysis; H.Q. and J.S. provided some experimental equipment; W.X. and X.X. provided technical support and all authors contributed to editing the manuscript. All authors have read and agreed to the published version of the manuscript.

Funding: This work was funded by the National Natural Science Foundation of China, grant number 62005094; Natural Science Foundation of Shandong Province, grant number ZR2021MF128; Industrial Chain Program of Shandong Laser Equipment Innovation and Entrepreneurship Community, grant number JGCYL2022−5 and Doctoral Fund Project from University of Jinan, grant number XBS1917.

Institutional Review Board Statement: Not applicable.

Informed Consent Statement: Not applicable.

Data Availability Statement: Not applicable.

Conflicts of Interest: The authors declare no conflict of interest.

References

1. Witte, U.; Traub, M.; Di Meo, A.; Hamann, M.; Rubel, D.; Hengesbach, S.; Hoffmann, D. Compact 35 μm fiber coupled diode laser module based on dense wavelength division multiplexing of NBA mini-bars. High-Power Diode Laser Technology and Applications XIV. *SPIE* **2016**, *9733*, 83–94.
2. Ma, X.; Zhang, N.; Zhong, L.; Liu, S.; Jing, H. Research progress of high power semiconductor laser pump source. *High Power Laser Part. Beams* **2020**, *32*, 121010.
3. Cao, C.; Wang, X.; Zeng, X.; Pan, Z.; Luo, L.; Cheng, Y. The problem with beam quality for semiconductor laser. *Optik* **2016**, *127*, 3701–3702.
4. Miah, M.; Strohmaier, S.; Urban, G.; Bimberg, D. Beam quality improvement of high−power semiconductor lasers using laterally inhomogeneous waveguides. *Appl. Phys. Lett.* **2018**, *113*, 221107. [CrossRef]
5. Ren, T.; Wu, C.; Yu, Y.; Dai, T.; Chen, F.; Pan, Q. Development Progress of 3–5μm Mid−Infrared Lasers: OPO, Solid-State and Fiber Laser. *Appl. Sci.* **2021**, *11*, 11451. [CrossRef]
6. Ebert, C.; Guiney, T.; Irwin, D.; Patterson, S. New advancements in 793 nm fiber−coupled modules for Th fiber laser pumping, including packages optimized for low SWaP applications. *SPIE* **2016**, *9834*, 102–110.
7. Lancaster, D.; Sabella, A.; Hemming, A.; Bennetts, S.; Jackson, S. *Power-Scalable Thulium and Holmium Fibre Lasers Pumped by 793 nm Diode-Lasers*; Optical Society of America: Washington, DC, USA, 2007.
8. Hemenway, M.; Chen, Z.; Kanskar, M.; Urbanek, W.; Dawson, D.; Bao, L. Wavelength stabilized fiber−coupled laser modules for DPSS and fiber laser pumping. *SPIE* **2020**, *11262*, 101–109.
9. Liu, G.; Lehkonen, S.; Li, J.; Winhold, H.; Rothacker, T.; Ahmed, F.; Peters, M.; Wolf, P.; Ahlert, S.; Kissel, H.; et al. High power and reliable 793nm T−bar and single emitter for thulium-doped fiber laser pumping. *SPIE* **2020**, *11262*, 51–59.
10. Hasler, K.; Wenzel, H.; Crump, P.; Knigge, S.; Maasdorf, A.; Platz, R.; StaskE, R.; Erbert, G. Comparative theoretical and experimental studies of two designs of high−power diode lasers. *Semicond. Sci. Technol.* **2014**, *29*, 045010. [CrossRef]
11. Lee, J.; Mawst, J.; Botez, D. Asymmetric broad waveguide diode lasers (λ = 980 nm) of large equivalent transverse spot size and low temperature sensitivity. *IEEE Photonics Technol. Lett.* **2002**, *14*, 1046–1048. [CrossRef]
12. Tomm, W.; Ziegler, M.; Hempel, M.; Elsaesser, T. Mechanisms and fast kinetics of the catastrophic optical damage (COD) in GaAs−based diode lasers. *Laser Photonics Rev.* **2011**, *5*, 422–441. [CrossRef]
13. Wang, Z.; Koenning, T. Fiber coupled diode laser beam parameter product calculation and rules for optimized design. *SPIE* **2011**, *7918*, 86–94.
14. Ren, Z.; Li, Q.; Li, B.; Song, K. High wall-plug efficiency 808-nm laser diodes with a power up to 30.1 W. *J. Semicond.* **2020**, *41*, 61–63. [CrossRef]

15. Kanskar, M.; Bao, L.; Bai, J.; Chen, Z.; Dahlen, D.; Devito, M.; Dong, W.; Grimshaw, M.; Guan, X. High reliability of high power and high brightness diode lasers, High−Power Diode Laser Technology and Applications XII. *SPIE* **2014**, *8965*, 52–61.
16. Bao, L.; Kanskar, M.; DeVito, M.; Hemenway, M.; Urbanek, W.; Grimshaw, M.; Chen, Z.; Dong, W.; Guan, X.; Zhang, S.; et al. High reliability demonstrated on high-power and high-brightness diode lasers. *SPIE* **2015**, *9348*, 88–97.